J|A|C|S ARTICLES

Published on Web 03/22/2010

Directed Self-Assembly of Dipeptides to Form Ultrathin Hydrogel Membranes

Eleanor K. Johnson,[†] Dave J. Adams,[‡] and Petra J. Cameron*,[†]

Department of Chemistry, University of Bath, BA2 7AY, United Kingdom, and Department of Chemistry, University of Liverpool, L69 7ZD, United Kingdom

Received November 11, 2009; E-mail: p.j.cameron@bath.ac.uk

Abstract: The dipeptide amphiphile Fmoc-Leu-Gly-OH has been induced to self-assemble into thin surface-supported hydrogel gel films and gap-spanning hydrogel membranes. The thickness can be closely controlled, giving films/membranes from tens of nanometers to millimeters thick. SEM and TEM have confirmed that the dipeptides self-assemble to form fibers, with the membranes resembling a dense "mat" of entangled fibers. The films and membranes were stable once formed. The films could be reversibly dried and collapsed, then reswollen to regain the gel structure.

Introduction

Peptide-based hydrogels are being investigated for a wide range of applications in the fields of health care and advanced materials;[1] of particular interest are a subset of peptide hydrogels that are formed from amino acids or dipeptides.[2−6] These small amphiphilic molecules self-assemble to form supramolecular gels, with scanning electron microscopy showing a fibrous structure on the nanometer scale.[2,7] These gels are not cross-linked in the conventional sense; the structure appears to be solely due to entanglement of the fibers formed by noncovalent forces such as hydrogen bonding and $\pi-\pi$ stacking between peptides.[8−10] A variety of dipeptides will self-assemble into hydrogel matrices. In particular *N*-protected dipeptides (Fmoc, Boc, Cbz, or naphthalene protected) and constrained dipeptides (such as Phe−Phe dimers with unsaturation at one of the α-carbons) have been investigated.[11−18] Gelation is induced by pH change,[9,17] solvent polarity changes,[12] or enzyme action.[14,16] These materials are of interest as biomimetic extracellular environments and have shown promise as 3-D scaffolds for cell culturing.[11,13,19] The materials are also being studied as agents for tissue repair,[3] as supports for enzymes and artificial enzymes for aqueous catalysis,[10,16] as scaffolds for sensing, and as tunable materials for drug delivery.[4,15]

The size and shape of the dipeptide hydrogel is typically dictated by the size and shape of the container in which it is formed. The ability to prepare thin films of dipeptide hydrogel would introduce a range of new applications, for example the ability to create thin supported layers for specific cell attachment or biomedical applications.[20] Surface-initiated growth opens the possibility of preparing multilayered structures, where gel layers with different properties are grown sequentially.

The preparation of thin polymer hydrogel films has previously been carried out by polymerization between two glass plates[21] and by plasma polymerization.[22] Polysaccharides have been formed into films on an electrode by electrophoresis.[23−26] Thin hydrogel films of assembled peptides have been prepared by spraying solutions onto surfaces.[27] Electrochemistry has been widely used to chemically change molecules grafted to an

[†] University of Bath.
[‡] University of Liverpool.

(1) Mohammed, J. S.; Murphy, W. L. *Adv. Mater.* **2009**, *21*, 2361–2374.
(2) Ulijn, R. V.; Smith, A. M. *Chem. Soc. Rev.* **2008**, *37*, 664–675.
(3) Hirst, A. R.; Escuder, B.; Miravet, J. F.; Smith, D. K. *Angew. Chem., Int. Ed.* **2008**, *47*, 8002–8018.
(4) (a) Sutton, S; Campbell, N. L.; Cooper, A. I.; Kirkland, M.; Frith, W. J.; Adams, D. J. *Langmuir* **2009**, *25*, 10285–10291. (b) Chen, L.; Morris, K.; Laybourn, A.; Elias, D.; Hicks, M. R.; Rodger, A.; Serpell, L. C.; Adams, D. J. *Langmuir* **2010**, DOI: 10.1021/la903694a. (c) Adams, D. J.; Mullen, L. M.; Berta, M.; Frith, W. F. *Soft Matter*, DOI:10.1039/b921863g.
(5) Yang, Z. M.; Liang, G. L.; Ma, M. L.; Gao, Y.; Xu, B. *J. Mater. Chem.* **2007**, *17*, 850–854.
(6) Liang, G. L.; Yang, Z. M.; Zhang, R. J.; Li, L. H.; Fan, Y. J.; Kuang, Y.; Gao, Y.; Wang, T.; Lu, W. W.; Xu, B. *Langmuir* **2009**, *25*, 8419–8422.
(7) Panda, J. J.; Mishra, A.; Basu, A.; Chauhan, V. S. *Biomacromolecules* **2008**, *9*, 2244–2250.
(8) Banerjee, A.; Palui, G.; Banerjee, A. *Soft Matter* **2008**, *4*, 1430–1437.
(9) Mahler, A.; Reches, M.; Rechter, M.; Cohen, S.; Gazit, E. *Adv. Mater.* **2006**, *18*, 1365–1370.
(10) Smith, A. M.; Williams, R. J.; Tang, C.; Coppo, P.; Collins, R. F.; Turner, M. L.; Saiani, A.; Ulijn, R. V. *Adv. Mater.* **2008**, *20*, 37–41.
(11) Wang, Q.; Yang, Z.; Ma, M.; Chang, C. K.; Xu, B. *Chem.—Eur. J.* **2008**, *14*, 5073–5078.
(12) Jayawarna, V.; Smith, A.; Gough, J. E.; Ulijn, R. V. *Biochem. Soc. Trans.* **2007**, *35* (3), 535–537.
(13) Yan, X.; Cui, Y.; He, Q.; Wang, K.; Li, J. *Chem. Mater.* **2008**, *20*, 1522–1526.
(14) Liebmann, T.; Rydholm, B.; V.; Akpe, V.; Brismar, H. *BMC Biotech.* **2007**, *7*, 88.
(15) Toledano, S.; Williams, R. J.; Jayawarna, V.; Ulijn, R. V. *J. Am. Chem. Soc.* **2006**, *128*, 1070–1071.
(16) Bardelang, D.; Zaman, M. B.; Moudrakovski, I. L.; Pawsey, S.; Margeson, J. C.; Wang, Q.; Wu, X.; Ripmeester, J. A.; Ratcliffe, C. I.; Yu, K. *Adv. Mater.* **2008**, *20*, 4517–4520.
(17) Wang, Q.; Yang, Z.; Gao, Y.; Ge, L.; Wang, W.; Xu, B. *Soft Matter* **2008**, *4*, 550–553.
(18) Adams, D. J.; Butler, M. F.; Frith, W. J.; Kirkland, M.; Mullen, L.; Sanderson, P. *Soft Matter* **2009**, *5*, 1856–1862.
(19) Jayawarna, V.; Richardson, S. M.; Hirst, A.; Hodson, N. W.; Saiani, A.; Gough, J. E.; Ulijn, R. V. *Acta Biomater.* **2009**, *5*, 934–943.
(20) Takahashi, H.; Emoto, K.; Dubey, M.; Castner, D. G.; Grainger, D. W. *Adv. Funct. Mater.* **2008**, *18*, 2079–2088.
(21) Suri, J. T.; Cordes, D. B.; Cappuccio, F. E.; Wessling, R. A.; Singaram, B. *Angew. Chem.* **2003**, *115*, 6037–6039.
(22) Bhattacharyya, D.; Pillai, K.; Chyan, O. M.; Tang, L.; Timmons, R. B. *Chem. Mater.* **2007**, *19*, 2222–2228.

10.1021/ja909579p

Scheme 1. (a, Right) Schematic of the SPR Electrochemistry Cell for Combined SPR−Film Growth Experiments; (b, Left) Schematic of the Experimental Setup Used for Growing Gel Membranes That Spanned TEM Grids

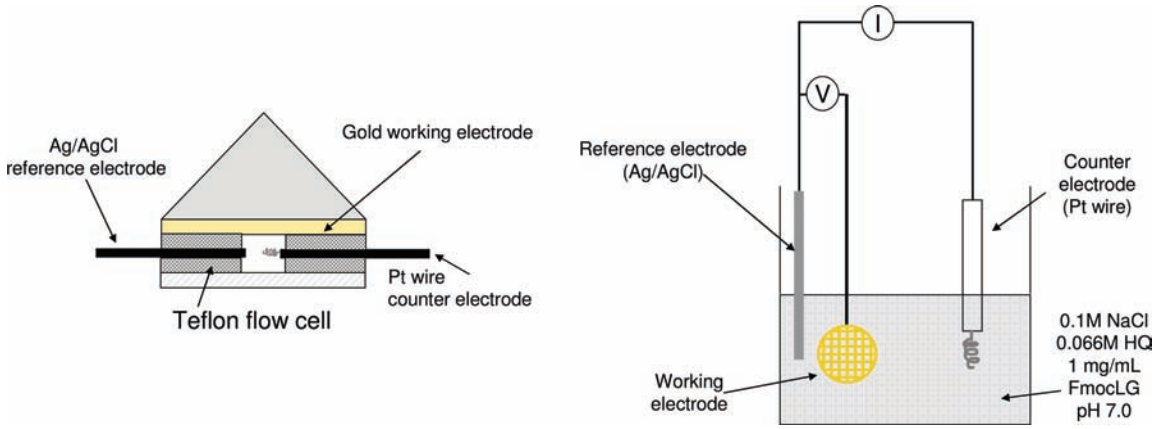

Scheme 2. (a) Fmoc-Leu-Gly-OH; (b) Electrochemical Two-Electron Oxidation of Hydroquinone[a]

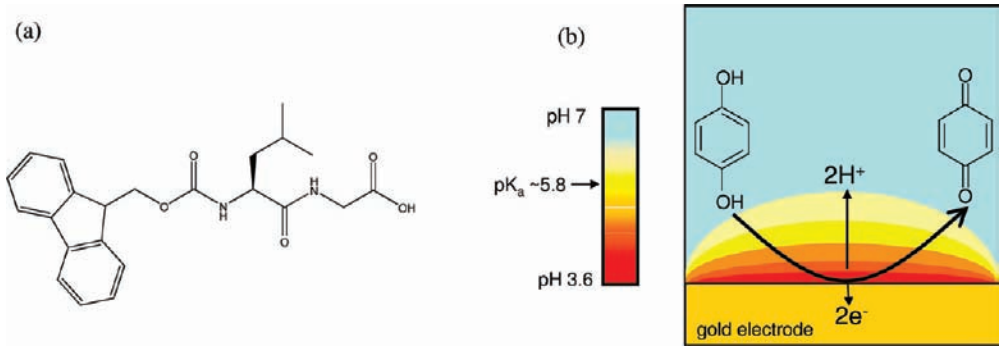

[a] When hydroquinone is oxidized to 1,4-benzoquinone, it releases two protons; the protons lower the pH close to the electrode surface and create a localized area where the pH is below the pK_a[4] of the Fmoc-Leu-Gly-OH. In the bulk Fmoc-Leu-Gly-OH gels below pH 4, at the surface this would translate to gelation within the dark red-orange diffusion layer above the electrode surface. Calculations of the pH drop induced at the electrode surface are included in the Supporting Information.

electrode surface. For example electrochemistry can be used to direct the surface attachment of oligonuleotides,[28] and hydroquinone oxidation has been used to carry out site-specific deprotection of organic molecules immobilized on microarrays.[29] Bohn et al. have used potential gradients to create variable thickness polyacrylic acid layers on gold electrodes;[30] they have also used voltage changes to control the degree of swelling in surface-grafted hydrogel films.[31]

In this paper, we report the electrochemically induced growth of thin self-assembled Fmoc-Leu-Gly-OH (Schemes 1 and 2) hydrogel films. Film growth was controlled by inducing a localized pH drop at an electrode surface by the oxidation of hydroquinone. Fmoc-Leu-Gly-OH has previously been shown to be an efficient low molecular weight hydrogelator.[18] It is demonstrated that gel membranes can be grown spanning 95 and 230 μm diameter holes in a metal grid, creating areas of thin free-standing membrane with water on both sides, which are more biologically relevant than solid gel blocks and could be used to study interactions with biomolecules or diffusion of small molecules through the gel.[21,32]

We also report the controllable growth of films or membranes with thicknesses from tens of nanometers to millimeters. Film growth can be stopped and started at will, and the films are stable once formed. Film growth is also reversible, with total disassembly occurring when the electrochemical growth conditions are reversed. The growth of films with thicknesses below 200 nm was followed in situ by surface plasmon resonance spectroscopy (SPR).[33] Gels were imaged using scanning electron microscopy (SEM), transmission electron microscopy (TEM), and confocal microscopy. Drying and swelling experiments were also carried out and showed the reversible collapse and rehydration of the films. To the best of our knowledge, this is the first report of the growth of hydrogel films and membranes with controllable thicknesses via peptide self-assembly.

Materials and Methods

A full explanation of the methods used in this paper are given in the Supporting Information. Briefly, thin gel films were grown

(23) Wu, L.; Gadre, A. P.; Yi, H.; Kastantin, M. J.; Rubloff, G. W.; Bentley, W. E.; Payne, G. F.; Ghodssi, R. *Langmuir* **2002**, *18*, 8620–8625.
(24) Wu, L.; Yi, H.; Li, S.; Rubloff, G. W.; Bentley, W. E.; Ghodssi, R.; Payne, G. F. *Langmuir* **2003**, *19*, 519–524.
(25) Yi, H.; Wu, L.; Ghodssi, R.; Rubloff, G. W.; Payne, G. F.; Bentley, W. E. *Langmuir* **2005**, *21*, 2104–2107.
(26) Yang, X; Shi, X.; Liu, Y.; Bentley, W. E.; Payne, G. F. *Langmuir* **2009**, *25*, 338–344.
(27) Haines-Butterick, L. A.; Salick, D. A.; Pochan, D. J.; Schneider, J. P. *Biomaterials* **2008**, *29*, 4164–4169.
(28) Egeland, R. D.; Marken, F.; Southern, E. M. *Anal. Chem.* **2002**, *74*, 1590–1596.
(29) Egland, R. D.; Southern, E. M. *Nucleic Acid Res.* **2005**, *33*, e125.
(30) Wang, X.; Haasch, R. T.; Bohn, P. W. *Langmuir* **2005**, *21*, 8452–8459.
(31) Lokuge, I. S.; Bohn, P. W. *Langmuir* **2005**, *21*, 1979–1985.
(32) Tokarev, I.; Minko, S. *Soft Matter* **2009**, *5*, 511–524.
(33) Knoll, W.; Kasry, A.; Yu, F.; Wang, Y.; Brunsen, A.; Dostalek, J. *J. Nonlinear Opt. Phys.* **2008**, *17* (2), 121–129.

directly on top of gold films. Self-supporting gel membranes were grown directly onto gold TEM sample grids; the gels formed continuous layers across both 95 and 230 μm diameter holes in the grids. To grow hydrogel films, a stock solution of 0.24 mol dm^{-3} (100 mg cm^{-3}) of Fmoc-Leu-Gly-OH (synthesized as described in ref 18) in DMSO was prepared. Then 10 μL of the stock was added to 1 cm^{-3} of a solution containing 0.066 mol dm^{-3} hydroquinone (Sigma-Aldrich, >99%) and 0.1 mol dm^{-1} NaCl (Sigma-Aldrich, ≥99.5%). Then 4 μL of 1 mol dm^{-3} NaOH (Sigma-Aldrich, ≥98%) was added to fully dissolve the dipeptide, and 8 μL of 1 mol dm^{-3} HCl (Sigma-Aldrich 36.5−38.0%) to bring the pH to 7.0. The final solution was introduced to the surface of the gold slide via an electrochemical flow cell.

The gold-coated LaSFN9 glass slide or the gold TEM grid acted as the working electrode in a three-electrode electrochemical cell. The cell was completed by a platinum counter electrode and an Ag^+/AgCl reference electrode (World Precision Instruments, Dri-Ref). The electrochemical growth of the Fmoc-Leu-Gly-OH films was induced galvanostatically (Ecochemie, Autolab PGSTAT 12) by applying a 20 μA cm^{-2} oxidation current for a desired length of time. The applied potential was in the range 0.36−0.38 V. Experiments were carried out in 0.1 M NaCl salt solution at pH 7. Galvanostatic control was used to ensure constant film growth. As the film grew, it was necessary to apply slightly higher voltages to maintain the constant electrochemical oxidation of hydroquinone. Gels were removed from the surface by passing a current of −10 μA cm^{-2} for 500 s.

Results and Discussion

Fmoc-Leu-Gly-OH (Scheme 2a) has been previously shown to form hydrogels at concentrations above 1.46 × 10^{-2} mol dm^{-3} (5.8 mg cm^{-3}) when the acidity is lowered below pH 4.[18] Gelation is induced by the addition of acid; it has been shown that both HCl and glucono-δ-lactone induce gelation, although the slow hydrolysis of glucono-δ-lactone in water to yield gluconic acid leads to the formation of more transparent and homogeneous gels. In this study, a solution of 1 mg cm^{-3} of Fmoc-Leu-Gly-OH was added to a NaCl solution containing hydroquinone. Instead of creating a bulk pH drop by the addition of acid to the solution, a surface-localized pH drop was induced by the electrochemical oxidation of 1,4-hydroquinone at an electrode. When 1,4-hydroquinone oxidizes, it forms 1,4-benzoquinone and two protons (Scheme 2b). The oxidation reaction therefore causes a rapid lowering of pH close to the electrode surface and induces gelation in a very small volume of the solution. In this way, it was possible to make thin films of gel. Electrochemical gelation allowed the number of protons generated to be precisely controlled. It also allowed the speed at which the pH dropped to be controlled. When 1,4-hydroquinone was oxidized at a planar electrode, a thin surface-supported film of gel could be created. When a metal grid was used as the electrode, the gel grew outward from the gold wires making up the grid until it filled in the holes between the wires and created a film with areas of gap-spanning peptide membrane.

The oxidation of 1,4-hydroquinone was done galvanostatically, a method where the amount of current flowing at the electrode is controlled with time. The properties of the gel films appeared to be very dependent on the speed at which the localized pH drop was created. A graph relating gel density to growth conditions is shown as Figure 1 of the Supporting Information. The pH drop was controlled by the magnitude of the current that was allowed to flow at the electrode. When currents below 12 μA cm^{-2} were applied, gels did not form. The application of 20 μA cm^{-2} led to the formation of transparent gels that were stable when the surface was inverted.

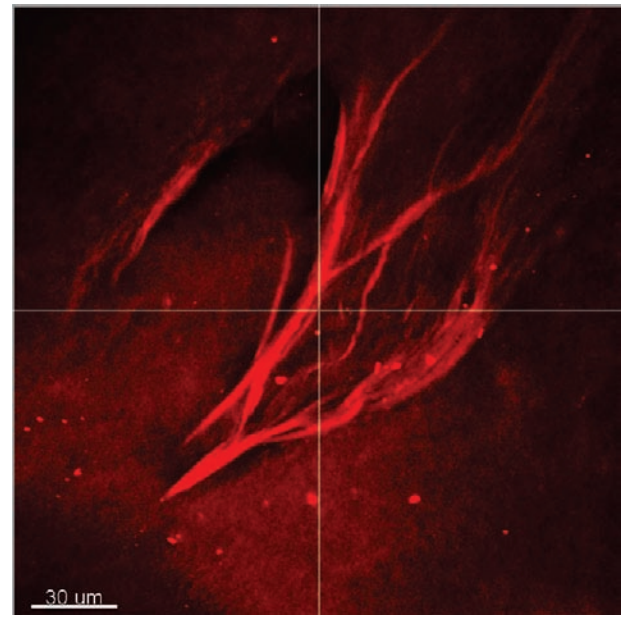

Figure 1. Confocal microscope image of a wet gel layer stained with nile red. The presence of fibers, as well as some spherical aggregates, can be seen.

The application of currents above 28 μA cm^{-2} led to the formation of nonhomogeneous lumpy gels that looked opaque rather than transparent. The longer the current was applied, the denser the gel became. These observations were supported by surface plasmon resonance spectroscopy (SPR) measurements. SPR is a surface-specific technique that can be used to measure mass changes at the surface of a gold film.[33] In this report electrochemistry and SPR were combined so that the electrochemically induced growth of the hydrogel film could be directly related to the change in mass at the gold surface. SPR allowed real-time information about gel growth to be extracted and is discussed in more detail later.

FTIR spectra of gel films grown directly onto gold electrodes indicated the presence of both β-sheets and β-turns in the self-assembled peptide structures (Supporting Information, Figure 2). The hydrogel films were further characterized by confocal microscopy and cryo-SEM. The gap-spanning membranes were characterized by TEM.

Figure 1 shows a confocal microscope image of a gel film grown on a fluorine-doped tin oxide coated microscope slide. In the first instance thick layers (∼1 mm) were grown to show proof of principle. The gel films were transparent and sufficiently robust to retain their shape after inversion, as with hydrogels prepared by conventional pH adjustment.[10,18] SEM, TEM, and confocal microscopy confirmed the presence of peptide fibrils in the gel. A cryo-SEM image of the top surface of a gel is shown in Figure 2. It is extremely difficult to obtain images of aqueous gels, as the (freeze) drying process often introduces artifacts. Freezing induces crystallization of water in the gel and the alignment of gel fibers between the crystals. Drying can also introduce artifacts as the gel agglomerates to reduce surface tension. In this paper SEM, TEM, and confocal microscopy of wet gels are all shown to build up a picture of the self-assembled films in a variety of environments. It is encouraging that all three techniques show the presence of fibers in the gel. Further structure in the images is not discussed to avoid drawing conclusions based on artifacts.

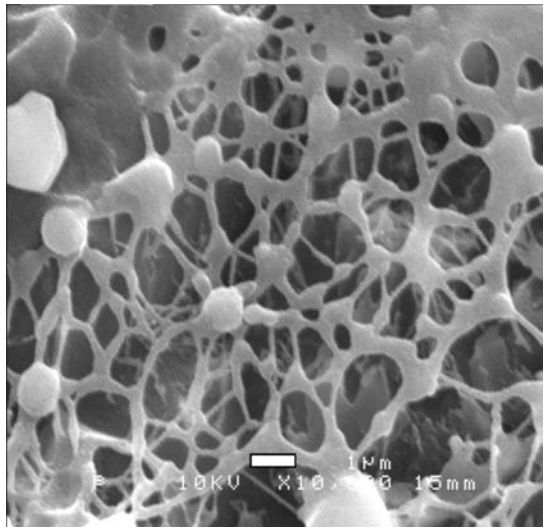

Figure 2. Cryo-SEM image of the top surface of an electrochemically grown gel film. The scale bar is 1 μm.

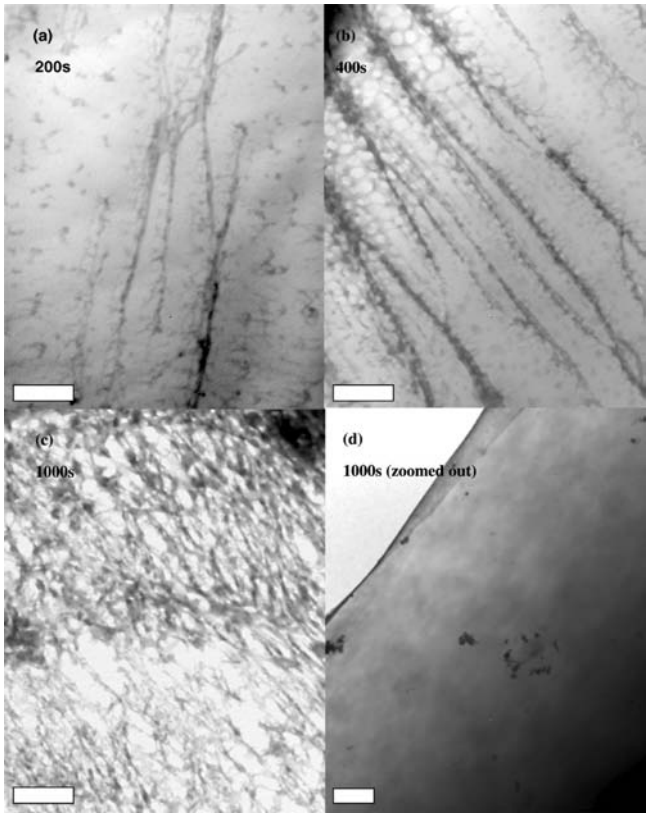

Figure 3. (a) TEM image of a gel grown by the application of 11.5 μA cm^{-2} for 200 s.The image shows the start of fiber formation, as well as some small aggregates in the film. The film is continuous, so the fibers are suspended in nanostructure below the resolution of the TEM. The scale bar is 0.5 μm. (b) TEM image of a film grown by the application of 11.5 μA cm^{-2} for 400 s. Fiber development can be seen. The scale bar is 0.5 μm. (c) TEM image of a film grown by the application of 11.5 μA cm^{-2} for 1000 s. The film now appears to be entirely composed of intertwining fibers. The scale bar is 0.5 μm. (d) Zoomed out TEM image of a film grown by the application of 11.5 μA cm^{-2} for 1000 s. The white area in the top left-hand corner of the image is free space, created when the membrane was torn. A picture of a torn membrane was chosen, as it clearly shows the thin gel layer, which has folded back upon itself along the line of the break. The scale bar is 2 μm.

In the case of the gap-spanning membranes, thin gap-spanning films were grown directly onto gold sample grids, dried in air, and then imaged by TEM. The membranes spanned 95 and 230 μm diameter holes (200 mesh and 50 mesh) in the gold grids. By growing the films on grids it was possible to study both the top and bottom surface of the gap-spanning membranes, which were indistinguishable from each other by TEM. A systematic study was undertaken to relate the length of time the current was allowed to flow to the resulting gel structure. TEM images of gels grown by the application of 11.5 μA cm^{-2} for 200, 400, and 1000 s are shown in Figure 3.

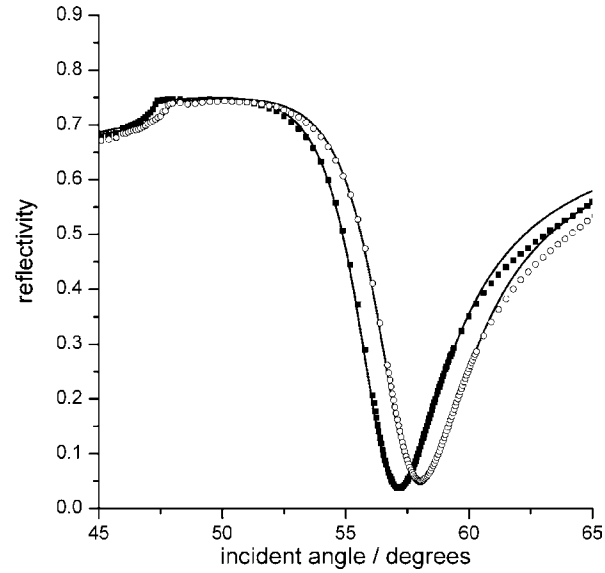

Figure 4. SPR scans showing the intensity of reflected light as a function of incident angle. The experimental data are given by the open symbols; the fit to a three-layer Fresnel model (Table 1) is given by the solid lines. The black squares show the SPR curve for a gold film precursor solution (before gelling). The open circles show the SPR curve for a gold film with a thick (~1 mm) gel layer on the gold surface. The critical angle, Θ_C, shifts from 47.4° to 47.8°. The gel layer extends well beyond the 200 nm sensing range of the evanescent surface plasmon wave. The surface plasmon wave therefore sees the gel as an infinite layer with a dielectric constant of 1.789. The parameters used for fitting are outlined in Table 1.

Table 1. Parameters and Values Used to Fit the SPR Scans Shown in Figure 4

layer	thickness/nm	ε(real)	ε(imaginary)
prism	∞^a	3.39	0
gold	51.15	−11.99	1.5016
air	∞	1.0016	0
precursor solution	∞	1.77	0
gel	∞^b	1.789	0.002

[a] Infinite thickness implies a layer that is much thicker than the evanescent tail of the surface plasmon wave. [b] Thickness was considered infinite for layers > 500 nm.

In the case of nanometer-thick films grown on planar gold electrodes, growth was monitored in situ by SPR. SPR is a technique where laser light is used to excite surface plasmon resonances in a thin gold film. The exponentially decaying tail of the surface plasmon extends several hundred nanometers beyond the gold film into the dielectric medium and is very sensitive to small changes in refractive index within ~200 nm of the gold surface.[33,34] Changes in dielectric constant can be directly related to changes in mass at the gold surface. As a result, it is possible to monitor the growth of very thin films (<200 nm thick) using SPR. It is important to point out that

(34) Knoll, W. *Annu. Rev. Phys. Chem.* **1998**, *49*, 569–638.

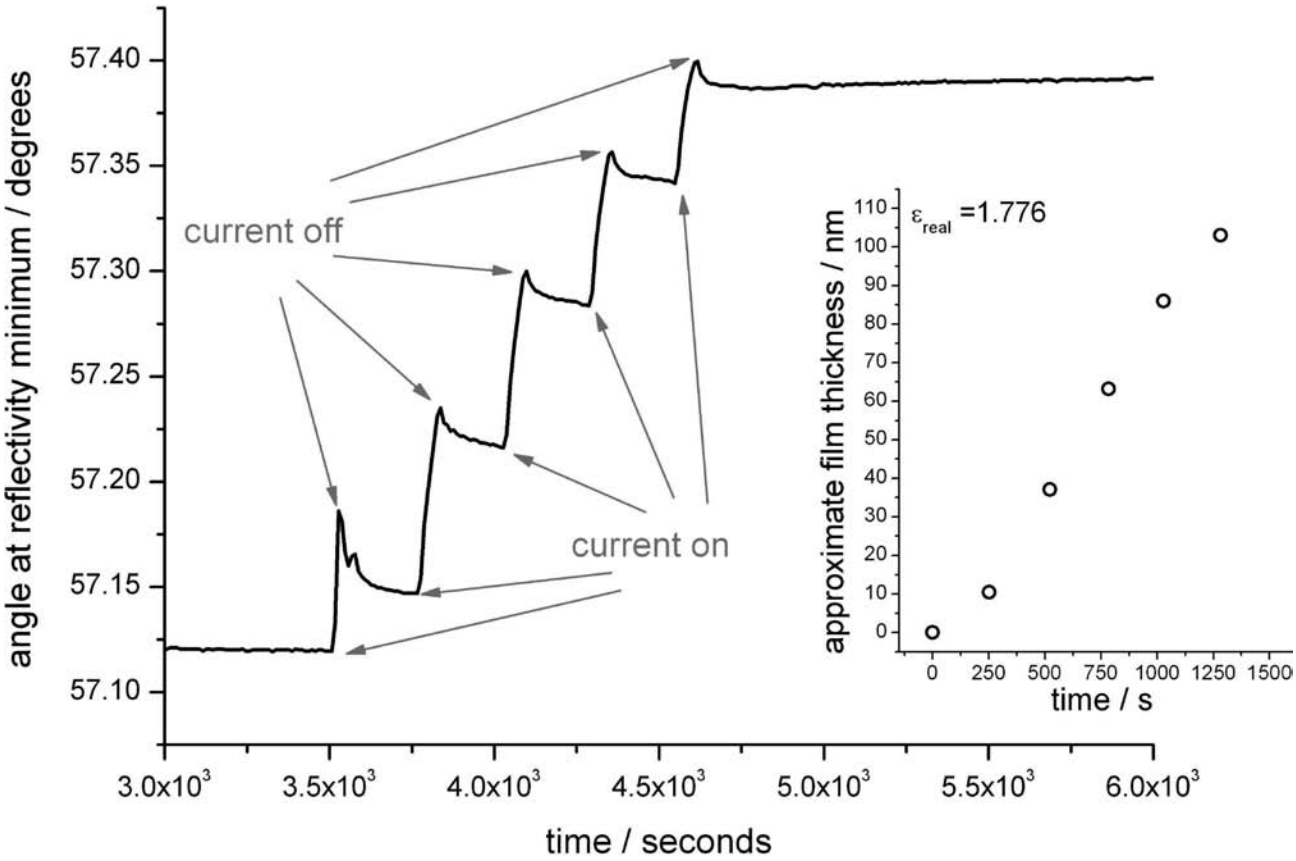

Figure 5. SPR experiment showing the stepwise growth in dipeptide film with each 60 s current pulse. A 200 s rest period was allowed between pulses. The total time the current was applied was 300 s. The inset shows the calculated growth in film thickness at the end of each 200 s rest period. The film thickness is approximate, as it was extremely hard to measure an accurate refractive index for the gel (depended on time of deposition and speed of deposition). The real values could vary by 10−20 nm from those given here.

SPR will measure only changes in thickness of films that are within the evanescent tail of the surface plasmon. Once the film extends beyond the evanescent tail, SPR can be used to measure only the bulk refractive index of the hydrogel layer. Figure 4 shows surface plasmon resonance spectra for a gold film in aqueous solution (containing 2.44×10^{-3} mol dm^{-3} Fmoc-Leu-Gly-OH and 0.066 mol dm^{-3} hydroquinone in a 0.1 M solution of NaCl) and the same gold film after a ∼1 mm thick hydrogel film had been grown on the surface. When a surface plasmon is excited in a gold film, a sharp dip in the reflectivity is seen. The position of both the reflectivity minimum and the critical angle is indicative of the dielectric properties of any layers above the gold surface (see Figure 4).[34] In the precursor solution, the critical angle occurred at 47.4° and the minimum at 57.2°. When a 1 mm gel layer was grown on the surface, the critical angle was 47.8° and the minimum was 58.1°. The dielectric constants of the films were obtained by carrying out Fresnel fitting of the SPR curves using commercially available software.[35] The Fresnel model is used in ref 31 to describe nanometer dimension poly(hydroxyethyl methacrylate) hydrogels and is a good approximation for isotropically nanostructured thin films. A four-layer model of glass||gold||hydrogel||water (or air) was used. Fresnel modeling of the thin hydrogel layers was used to extract layer thickness. This model can be used to calculate layer thickness only when the hydrogel film is <200 nm thick (i.e., it is thinner than the evanescently decaying surface plasmon tail). In the case of hydrogel layers thicker than 200 nm, they were modeled as infinite superstrate layers. This means that they are modeled in exactly the same way as air or solvent above a gold film, and it is assumed that the decaying surface plasmon wave experiences a single dielectric environment. In the case of the thicker films the fit was used qualitatively to obtain the refractive index of the gel (from this value the water content of the gel could be estimated under different growth conditions; see Figure 1 in the Supporting Information). The fitting parameters are outlined in Table 1. The fits are given by the solid lines in Figure 4.

The dielectric constant of the 1 mm hydrogel film was found to be just slightly higher than that of water. The dielectric constant for the precursor solution was taken as ε(real) = 1.77 and ε(imaginary) = 0 (λ = 632.8 nm).[36] The fully formed (1 mm thick) hydrogel was found to have a dielectric constant of ε(real) = 1.789 and ε(imaginary) = 0.002. The calculated value of the film dielectric constant confirmed the formation of an open aqueous gel network with a dielectric constant close to that of water; for comparison, a dense layer of polypeptide on a surface typically has a much higher dielectric constant of ε(real) between 2.0 and 2.25.[37,38] The small imaginary component of the dielectric constant can be caused by either scattering or absorption.[39−41] As the peptide gel does not absorb at 632.8 nm, it is likely that the curve broadened due to

(35) *Winspall* fitting software; Res-Tec, Resonant Technologies GmbH: Framersheim, Germany.

(36) Cameron, P. J.; Jenkins, A. T. A.; Knoll, W.; Marken, F.; Milsom, E. V.; Williams, T. L. *J. Mater. Chem.* **2008**, *18*, 4304–4310.
(37) Lau, K. H. A.; Duran, H.; Knoll, W. *J. Phys. Chem. B* **2009**, *113*, 3179–3189.
(38) Savchenko, A.; Kashuba, E.; Kashuba, V.; Snopok, B. *Anal. Chem.* **2007**, *79*, 1349–1355.

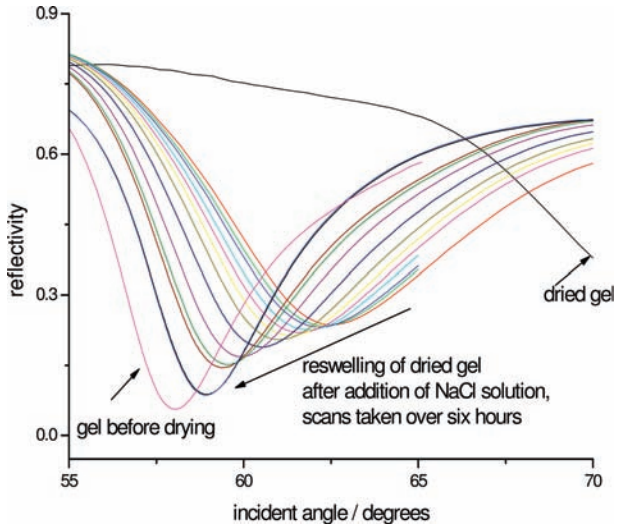

Figure 6. The pink curve shows the SPR scan of a freshly formed gel layer. The film in the SPR cell was dried under vacuum overnight. After drying, the minimum of the SPR curve shifted to an angle ≫ 70° (black curve). The curve also broadened, and an increase of the reflectivity at the minimum was seen. The shift to higher angles is caused by the collapse of the gel on the surface, leading to a more compact film with a higher refractive index (the collapsed film was several hundred micrometers thick). The broadening and the increase in the reflectivity minimum were due to the collapsed gel scattering the light to a much greater degree due to the presence of structure on the length scale of the wavelength of the light. Indeed when compared to the swollen gel, the collapsed film appeared to be translucent rather than transparent. On addition of 0.1 mol dm^{-3} of NaCl solution at pH 7, the film was observed to swell and to become more transparent, as evidenced by the shift to the right of the minimum angle and the narrowing of the peaks. After 6 h the blue curve was measured for the reswollen gel, just to the right of the "as-formed" gel.

scattering when structures/roughness on the length scale of the light were formed during the self-assembly process. In the case where the growth of films thinner than 200 nm was followed, no imaginary component of the spectrum was seen, suggesting that at this short time the film structure is too small to scatter the light. This observation is supported by the TEM images shown in Figure 3.

SPR allowed the fine control that electrochemical growth gave over the film thickness to be demonstrated. Figure 5 shows a kinetic scan where film growth was monitored in real time by following the change in the reflectivity minimum as the gel was formed. The change in reflectivity minimum gives real-time information on the dielectric constant and the thickness of the growing film. As long as the film thickness is less than 200 nm, it is a good measure of film growth. To show the control over film thickness provided by electrochemical film generation, 20 μA cm^{-2} was applied for 60 s and the film stability monitored over a 200 s rest period. Figure 5 shows the increase in reflectivity, and hence film thickness, as 60 s current pulses were applied. The inset shows the change in film thickness calculated by measuring how much the dielectric properties of the film changed at the end of each 200 s rest period. A ∼20 nm increase for every 60 s application of 20 μA cm^{-2} was observed. The film thickness was calculated by the fitting software using a dielectric constant of 1.776 for the film. The dielectric constant/refractive index of all gel films reported in this paper were obtained by fitting angular SPR scans taken before and after gel deposition. As a result, they are specific to each film. The film grown in Figure 5 had a lower dielectric constant than the thicker film measured by SPR in Figure 4 (1.776 compared to 1.789). This is believed to be due to the fact that the film was grown for a short time and a complex/dense fibrous structure had not yet developed. Figures 1 and 3 in the Supporting Information show that changes in the length of time the current is applied and in the total current passed lead to systematic changes in the dielectric constant (and therefore density/composition) of the film. A single value of the dielectric constant for all gel films is not quoted, as the structure and density of the films are very dependent on the growth conditions.

At short times some material was lost from the surface after the current was switched off. This is likely to be due to the fact that only a small pH change was generated after 60 s and the protons rapidly diffused away from the electrode. As the experiments are in pH 7 solution, the pH will therefore start to increase once the current is switched off and some of the gel will dissolve from the surface. As the current is applied and the pH lowered for longer times, a more stable and "intertwined" gel is formed (see TEM images in Figure 3) and the films became much more stable on the surface. Stopping the experiment and removing the gold slide from the flow cell after the 60 s current steps resulted in a stable surface-supported layer. When the layer was left in the electrochemical flow cell and a current of −10 μA cm^{-2} was applied for 500 s (protons were consumed), the film dissolved completely from the gold surface and the minimum angle in the SPR curve returned to the position for the precursor solution.

After formation, several films were dried under vacuum in the SPR cell. During drying, the films collapsed on the surface of the gold substrate and appeared translucent. SPR of dry films showed a large increase in dielectric constant, consistent with the film collapsing into a dense layer on the gold surface. Once the films were dry, the SPR cell was refilled with 0.1 mol dm^{-3} NaCl solution at pH 7, and the reswelling of the gel film was monitored in situ. Reswelling for a thick (∼0.5 mm when collapsed) film is shown in Figure 6. Over six hours, the SPR curves moved back to lower angles and approached the curve of the "as-formed" gel. The reswelling did not result in an identical curve to the "as-formed" gel, but a transparent layer of hydrogel was visually observed on the surface after the measurement was complete. In the case of thinner (∼100 nm) films, reswelling occurred over ∼160 min and resulted in a SPR curve almost identical to the "as-formed" curve.

Several other interesting observations of electrochemically generated Fmoc-Leu-Gly-OH films should be noted. In the presence of hydroquinone, gels formed at applied voltages of between 0.34 and 0.36 V. In the absence of hydroquinone and in acidic solution at pH 5.5, gel layers formed at potentials positive of 1.3 V due to the formation of oxides on the gold surface and the release of protons. Hydroquinone was used in these studies, as it lowered the required voltage considerably and did not damage the gold surface. It was also more reproducible, as the concentration of hydroquinone and H^+ could be closely controlled. A second interesting observation was that if a thin hydrogel layer was formed by applying 20 μA cm^{-2} for 100 s, and the thin film was then left in the precursor-containing solution, a thicker hydrogel layer would grow spontaneously out from the surface over several hours. The process was followed by SPR. In the absence of the initial 100 s application of current, no film grew on the surface. A 100 s

(39) Yu, F.; Ahl, S.; Caminade, A.; Majoral, J.; Knoll, W.; Erlebacher, J. *Anal. Chem.* **2006**, *78*, 7346–7350.
(40) Ekgasita, S.; Tangcharoenbumrungsuka, A.; Yu, F.; Baba, A.; Knoll, W. *Sens. Actuators, B* **2005**, *105*, 532–541.
(41) Cameron, P. J.; Zhong, X.; Knoll, W. *J. Phys. Chem. C* **2007**, *111*, 10313–10319.

application of 20 μA cm^{-2} (corrected for background non-Faradaic current) will generate a surface-localized pH of approximately 3.5 (see calculations in the Supporting Information). It may be that once the first layer of film is initiated there are sufficient protons present to slowly diffuse out of the film and initiate further film growth.

The pH drop at the electrode surface was calculated on the basis of the diffusion coefficient of H^+ [42] and the geometry of the electrode surface. The calculation showed that the pH drop required to initiate gelation at the surface is in line with the bulk pH drop required to form bulk gels by the addition of acid.[18]

Conclusions

The ability to grow films and membranes of gel in a controllable manner opens a range of new applications for dipeptide hydrogels. At present we are attempting to grow multilayer structures by the sequential deposition of different dipeptide moieties that gel under slightly different pH conditions, creating a 3-D structure with a range of different functionalities for immobilization of proteins or small molecules. The biomimicry of the gels could be investigated using free space spanning gel membranes, grown by initiating gelation on a metal grid.

The technique outlined here allows the rapid lowering of the pH in a known volume close to an electrode surface. By controlling the current and voltage applied, it is possible to change both the final pH and the speed at which the pH falls. The pH drop can also be reversed and the gel dissolved from the surface or simply halted to allow slow diffusion of protons into the solution and the growth of thicker hydrogel layers over several hours. The deposition conditions can be used to control the structure of the gel formed.

SPR has also been shown to be a useful method for studying the real-time growth of dipeptide films. Information can be obtained about the thickness and dielectric properties of the gels, with the future possibility of relating the dielectric constant to the density of gels formed from different dipeptides. SPR also allows changes in dielectric properties of the formed film to be monitored in situ over several hours and may contribute to the understanding of the evolution of peptide structures in the gel.

Acknowledgment. The authors thank Ursula Potter for help with SEM and TEM imaging.

Supporting Information Available: SPR studies relating preparation conditions to gel composition, FTIR of gel films, and the experimental conditions. This information is available free of charge via the Internet at http://pubs.acs.org.

JA909579P

(42) *CRC Handbook of Chemistry and Physics*, 77th ed.